

STEADY-STATE PHOTOCONDUCTIVITY OF AMORPHOUS (As₄S₃Se₃)_{1-x}Sn_x AND Ge_xAs_xSe_{1-2x} THIN FILMS

OXANA IASENIUC, MIHAIL IOVU

Institute of Applied Physics, Academy of Sciences of Moldova,

e-mail: oxana.iaseniuc@phys.asm.md

Received November 17, 2016

Abstract: In the present paper the experimental results on steady-state photoconductivity of amorphous (As₄S₃Se₃)_{1-x}Sn_x and Ge_xAs_xSe_{1-2x} thin films are presented and discussed. It was shown, that the spectral distribution of the stationary photoconductivity for both glass systems depends on the composition and polarity of the illuminated electrode. The experimental results are discussed in framework of the multiple trapping models for amorphous materials, with exponential distribution of the localized states in the band gap. The contact phenomenon appears at the interface between a metal electrode and an amorphous layer, what also is considered to be responsible for the peculiar features of photoelectric properties of investigated materials.

Key words: Chalcogenide glasses, amorphous thin films, coordination number, photoconductivity, localized states

1. INTRODUCTION

The Ge-As-Se and As-S-Se ternary glass systems actually attract a lot of attention because of their wide application in IR optics, non-linear optics, photonics, optoelectronics and as registration media for holography and e-beam lithography [1-4]. The physical properties of covalently-bonded glasses are determined by the mean coordination number Z (average number of covalent bonds per atom) [5]. It is well known that the functionality of many photonic and optoelectronic devices is based on the intrinsic photoelectric effect. From this point of view, investigations of stationary characteristic of photoconductivity of ternary amorphous thin films represent special interest. For the thermally deposited amorphous films, whose structure exhibits a higher level of disordered than the

bulk glasses, the incorporation of impurity atoms is more easily accessible, and in many cases the metal additives could become electrically active. The influence of Sn impurities on stationary and transient photoconductivity, and that was demonstrated at the example of amorphous $\text{As}_2\text{Se}_3\text{Sn}_x$ thin films [6-10]. It was demonstrated that introduction of Sn in the host material increases the drift mobility and the photosensitivity of the amorphous material. According to the ^{119}Sn Mössbauer spectroscopy in $\text{As}_2\text{Se}_3\text{Sn}_x$ glassy system [11], and X-ray photoelectron spectroscopy study of $\text{As}_x\text{Ge}_x\text{Se}_{1-2x}$ glasses [5], introduction of the elements such as Sn or Ge in arsenic selenide base glass, the new tetrahedral $\text{Sn}(\text{Se}_{1/2})_4$ and quasi-octahedral SnSe structural units, and GeSe_4 , respectively, can be formed. In this paper the experimental results of steady-state photoconductivity of amorphous $\text{Ge}_x\text{As}_x\text{Se}_{1-2x}$ and $(\text{As}_4\text{S}_3\text{Se}_3)_{1-x}\text{Sn}_x$ thin films are presented. It was observed that the dependence of light intensity on the steady-state photocurrent for all investigated amorphous thin films is non-linear, and is described by the expression $I_{ph} \sim F^\alpha$, where α takes the values $1.0 \leq \alpha \leq 0.5$, F is light intensity, I_{ph} is photocurrent. For Al- $\text{Ge}_x\text{As}_x\text{Se}_{1-2x}$ -Al thin film sandwich structure this dependence is sublinear ($\alpha \approx 0.5$), and is governed by bimolecular recombination. That means that the transport mechanism of the photo-excited carriers in investigated amorphous materials is attributed to the multiple trapping processes with exponential distribution of the localized states in the band gap [11]. For the investigated amorphous materials a energy diagram model with the probable group of localized states induced by the Sn and Ge in selenide base glass is proposed. Besides that, formation of metal-metal bonds and phase separation in the investigated $\text{Ge}_x\text{As}_x\text{Se}_{1-2x}$ and $(\text{As}_4\text{S}_3\text{Se}_3)_{1-x}\text{Sn}_x$ glasses can explain some physical-chemical properties [5].

2. EXPERIMENTAL

The bulk chalcogenide glasses $\text{Ge}_x\text{As}_x\text{Se}_{1-2x}$ ($x=0.05 \div 0.30$) and $(\text{As}_4\text{S}_3\text{Se}_3)_{1-x}\text{Sn}_x$ ($x=0 \div 0.10$) were prepared from the elements of 6N purity (As, S, Se, Ge, Sn) by conventional melt quenching method. Thin film samples of thicknesses $L=0.5 \div 17.5 \mu\text{m}$ were prepared by flash thermal evaporation in vacuum ($P=10^{-5}$ Torr) of the synthesized initial glasses onto glass substrates held at $T_{\text{substr}}=100^\circ\text{C}$. These samples have a sandwich configuration with two Al-electrodes, the one of which (top electrode) was transparent for the incident light. The dark conductivity σ_d , Lux-Ampere characteristics $I_{ph} = f(F)$ and the spectral distribution of stationary photocurrent $I_{ph} = f(\lambda)$ were measured in the constant current conditions using the spectrophotometer SPM-2 and the electrometrical amplifier U5-11, with the error less than $\pm 1.0\%$. The Lux-Ampere characteristics were investigated at the wavelength of the maximum photosensitivity of each sample, the light intensity

was varied by the calibrated neutral filters. All experiments were performed at room temperature ($\approx 20^\circ\text{C}$).

3. RESULTS AND DISCUSSION

Fig.1 represents the spectral distribution of photocurrent curves for Al-(As₄S₃Se₃)_{0.96}Sn_{0.04}-Al thin films structure at positive (+) and negative (-) polarity of applied field at the top Al illuminated electrode.

The different shape of these curves is caused by the contact phenomena between the interface of metallic electrode and the amorphous material and, as well as by the drift of the non-equilibrium carrier through the sample in the conditions of its multiple trapping on the localized states in the band gap of the disordered material. It was demonstrated that on the interface of the metallic electrode with the chalcogenide amorphous film is formed a potential barrier, the height of which depends on the nature of metal and amorphous material [12].

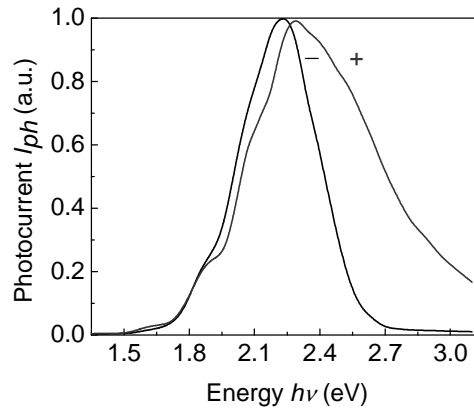


Fig.[1] Spectral distribution of the steady-state photocurrent for Al-(As₄S₃Se₃)_{0.90}Sn_{0.10}-Al thin film structure at positive (+) and negative (-) polarity applied to the top Al illuminated electrode.

It was also established that the value of the photocurrent is higher for the positive polarity from the Al-top irradiated electrode, and the maximum of the photocurrent is displaced toward higher photon energy region. This can be explained on the basis of contact phenomena between the interface of the metallic electrode and the amorphous film, as well as by the surface recombination processes.

For other compositions of amorphous thin films such as (As₄S₃Se₃)_{1-x}Sn_x, the shape of spectral distribution curves of photocurrent are similar.

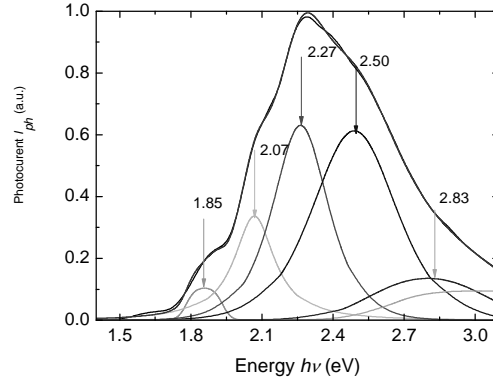


Fig.[2] Deconvoluted photocurrent spectrum using Gaussian function for Al-(As₄S₃Se₃)_{0.90}Sn_{0.10}-Al thin films structure at positive (+) polarity applied to the top Al illuminated electrode.

With increasing of Sn concentration in amorphous (As₄S₃Se₃)_{1-x}Sn_x thin films (up to $x=0.06$), the position of photocurrent maximum of which band gap value was determined according the Moss rule, is shifted to the lower energies, than, for higher concentrations (at $x \geq 0.06$) is slightly shifted to the higher energy, as was reported in [13, 14]

Fig.2 represents the results of deconvoluted photocurrent spectrum using Gaussian function for Al-(As₄S₃Se₃)_{0.90}Sn_{0.10}-Al thin films structure. The peak centered at $h\nu=2.27$ eV correspond to band-to-band photo-excitation of non-equilibrium carriers. The peaks situated around $h\nu=2.07$ eV and $h\nu=1.85$ eV can be attributed to some groups of localized levels induced by Sn impurities in the host chalcogenide glass. The observed peaks situated in the valence band around $h\nu=2.83$ eV for amorphous (As₄S₃Se₃)_{0.90}Sn_{0.10} thin films and around $h\nu=2.92$ eV for Ge_{0.07}As_{0.07}Se_{0.86} can be attributed to the electron states, which results predominantly from the *p*-orbital electron lone-pair of the chalcogen atoms and *p*- and σ -orbital states of chalcogen. In this approximation the shape of the spectra is governed by the short-range-order (SRO) [15].

Fig.3 represents the spectral distribution of the steady-state photocurrent for Al-Ge_xAs_xSe_{1-2x}-Al thin films structures at positive polarity applied at the top Al illuminated electrode. On the spectral curves of the steady-state photocurrent of the investigated structures were observed some peculiarities.

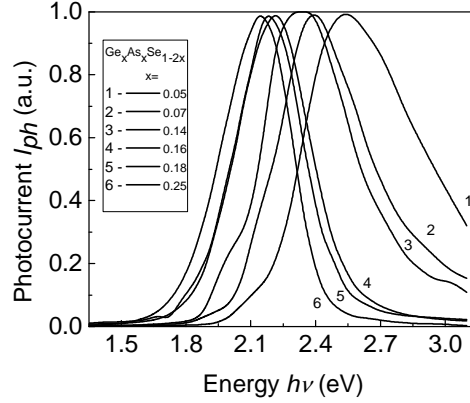


Fig.[3] Spectral dependence of the steady-state photocurrent for Al-Ge_xAs_xSe_{1-2x}-Al thin films structures at positive (+) polarity applied to the top Al illuminated electrode.

The peak centered at $h\nu=2.25$ eV correspond to band-to-band photo-excitation of non-equilibrium carriers. The peak situated around $h\nu=1.5$ eV for this composition, and the peaks observed at $h\nu=2.1$ eV, $h\nu=1.9$ eV, $h\nu=1.7$ eV, $h\nu=1.47$ eV, $h\nu=1.14$ eV for other compositions can be attributed to some groups of localized levels generated by tetrahedral Ge-based structural units in the host selenide glass.

Fig.4 represents the normalized curve of photocurrent for Al-Ge_{0.16}As_{0.16}Se_{0.68}-Al thin films structures at positive (+) polarity of applied field at the top Al illuminated electrode. For other Al-Ge_xAs_xSe_{1-2x}-Al thin film structures, as well as for all Al-(As₄S₃Se₃)_{1-x}Sn_x-Al planar structures, the shape of the curves of the spectral distribution of the steady-state photocurrent is similar. From the spectra of the steady-state photocurrent, the Moss rule was used for estimation of the band gap E_g values. According this method, the band gap E_g^{ph} corresponds to the value of the wavelength $\lambda_0 = \frac{1.24}{h\nu}$ at which the photocurrent fall down to a half value of it

maximum, as is shown in Fig.4. Some physical, optical and photoelectrical parameters of the investigated amorphous Ge_xAs_xSe_{1-2x} thin films (film composition x , the calculated mean coordination number Z , the optical band gap determined from Tauc plot E_g^{opt} , the refractive index n at $\lambda=0.7$ μm , the photoconductivity at the wavelength of the maximum of the photocurrent σ_{ph} , the energy of the maximum of the photocurrent $h\nu_{ph}^{max}$, the band gap determined from the spectra of the photocurrent according to Moss rule E_g^{ph} , the magnification of the photocurrent k_{ph}) are presented in Table 1 and selective in Fig.5.

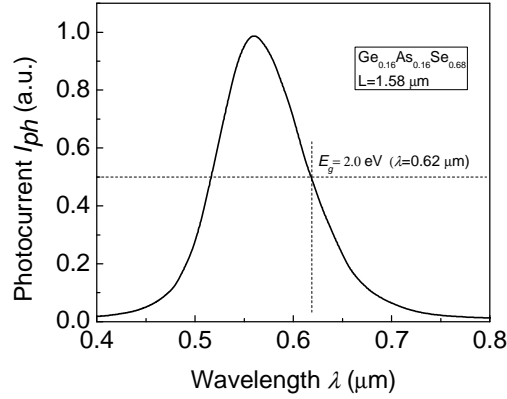


Fig.[4] Normalized curve of steady-state photocurrent for Al-Ge_{0.16}As_{0.16}Se_{0.68}-Al thin films structures at positive (+) polarity of applied field at the top Al illuminated electrode.

All investigated amorphous Ge_xAs_xSe_{1-2x} thin films have a light sensibility with the magnification of the photocurrent about $k_{ph} \sim 100$, and the dependence of optical parameters on the film composition is different for floppy, intermediate and stressed-rigide phases (Fig.5), as was demonstrated in the case of the experiments of the photocapacitance relaxation [16]. The Phillips-Thorpe thresholds versus average coordination number Z were reported by some authors in [17-20].

Table 1.
Some optical and photoelectrical parameters of amorphous Ge_xAs_xSe_{1-2x} thin films.

x	Z	E_g^{opt} (eV)	N ($\lambda=0.7 \mu m$)	$h\nu_{ph}^{max}$ (eV)	E_g^{ph} (eV)	K_{ph}
0.05	2.15	1.92	2.85	2.40	2.34	63
0.07	2.21	1.93	2.76	2.40	2.20	109
0.09	2.27	1.92	2.73	2.21	2.07	100
0.11	2.33	1.92	2.78	2.18	2.0	96
0.14	2.42	1.94	2.79	2.34	2.14	105
0.16	2.48	1.93	2.78	2.21	2.0	100
0.18	2.54	1.90	2.79	2.18	2.0	97
0.20	2.60	1.99	2.65	2.29	2.10	100
0.25	2.75	1.96	2.65	2.14	1.91	100
0.30	2.90	1.97	2.86	2.30	1.97	92

As was demonstrated in [5], from the experiments of high-resolution of X-ray photoelectron spectroscopy study, the topology of Ge_xAs_xSe_{1-2x} glasses evolves with increasing cation concentration (x) from the network consisting of separate

GeSe_{4/2} tetrahedra and AsSe_{3/2} pyramids interconnected via Se chains, towards the formation of structural fragments based on Ge-As, As-As and Ge-Ge bonds.

The trends of metal-metal bonds formation and subsequent phase separation can explain the observed peculiarities in compositional dependence of optical parameters, especially with some particularities for the compositions with $x=0.09$ ($Z=2.27$), $x=0.16$ ($Z=2.48$) and $x=0.25$ ($Z=2.75$).

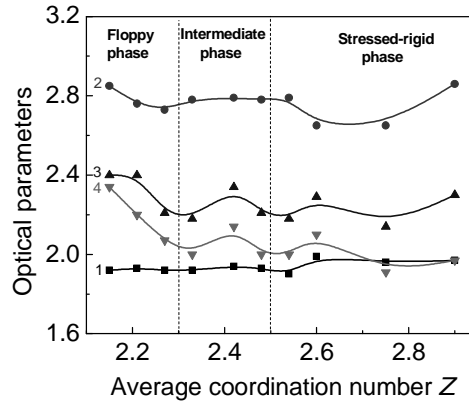


Fig.[5] Dependence of the optical parameters: 1-optical band gap E_g^{opt} (eV), 2-refractive index n (at $\lambda=0.7 \mu\text{m}$), 3- position of photocurrent maximum $h\nu_{ph}^{max}$ (eV), and 4- band gap E_g^{ph} (eV), determined according Moss rule for Al-Ge_xAs_xSe_{1-2x}-Al thin film structures versus average coordination number Z .

In Table 2 and Fig.6 are presented the dependencies of the optical parameters: 1-optical band gap E_g^{opt} (eV), 2-refractive index n (at $\lambda=0.7 \mu\text{m}$), 3- position of photocurrent maximum $h\nu_{ph}^{max}$ (eV), and 4- band gap E_g^{ph} (eV), determined according Moss rule for Al-(As₄S₃Se₃)_{1-x}Sn_x-Al thin film structures versus average coordination number Z . As in the case of amorphous Al-Ge_xAs_xSe_{1-2x}-Al thin film structures, these dependencies have non- monotonous character, but also have some peculiarities situated at different values of the average coordination number, which also can be explained by the structure of chalcogenide glass with different concentration of Sn.

Fig.7 represents the dependence of the steady-state photocurrent on the light intensity $I_{ph}=f(F)$ for all investigated amorphous Al-Ge_xAs_xSe_{1-2x}-Al thin films structures. The dependency of the steady-state photocurrent on the light intensity for all investigated amorphous Ge_xAs_xSe_{1-2x}-thin films is non-linear, and in the case of the exponential distribution of localized states in the band gap is described by the expression $I_{ph} \sim F^\alpha$, where α takes the values $0.5 \leq \alpha = \frac{T^*}{T + T^*} \leq 1.0$, where T^* - is the parameter of distribution of localized states [21].

Table 2.
Some optical and photoelectrical parameters of amorphous $(As_4S_3Se_3)_{1-x}Sn_x$ thin films.

x	Z	E_g^{opt} (eV)	n ($\lambda=0.7$ μm)	$h\nu_{ph}^{max}$ (eV)	E_g^{ph} (eV)	K_{ph}
0	2.400	1.82	2.51	2.45	2.18	250
0.01	2.416	1.78	2.69	2.40	2.04	100
0.03	2.448	1.78	2.77	2.28	2.12	100
0.04	2.464	1.77	2.73	2.37	2.06	100
0.05	2.480	1.74	2.74	2.13	1.92	100
0.06	2.496	1.75	2.72	2.18	1.91	100
0.07	2.512	1.74	2.71	2.14	1.90	100
0.09	2.544	1.71	2.86	2.21	1.99	100
0.10	2.560	1.72	2.71	2.22	2.04	100

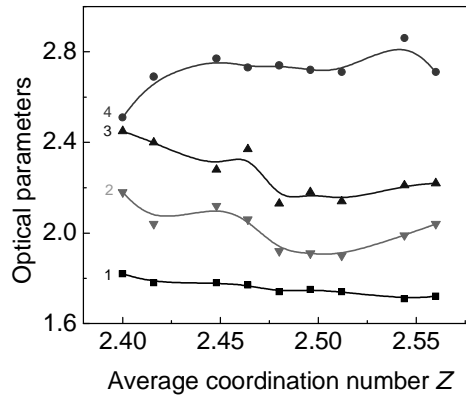


Fig.[6] Dependency of the optical parameters: 1-optical band gap E_g^{opt} (eV), 2-refractive index n (at $\lambda=0.7 \mu m$), 3- position of photocurrent maximum $h\nu_{ph}^{max}$ (eV), and 4- band gap E_g^{ph} (eV), determined according Moss rule for $Al-(As_4S_3Se_3)_{1-x}Sn_x-Al$ thin film structures versus average coordination number Z .

In the case when the transport mechanism of the photo-excited carriers in investigated amorphous materials is attributed to the multiple trapping processes with exponential distribution of the localized states in the band gap, the parameter α takes the values $0.5 \leq \alpha = \frac{2T^* - T}{T + T^*} \leq 2.0$ [22]. For $Al-Ge_xAs_xSe_{1-2x}-Al$ thin film structure this dependence is sublinear $\alpha \approx 0.7 \div 1.0$ in the region of low intensities and $\alpha \approx 0.5$ in the region of high intensities of the excited light (Fig.6). In Fig.7 the arrows indicate the mono- to bimolecular transition, as was demonstrated for

amorphous $\text{Ge}_x\text{Se}_{100-x}$ thin films [23].

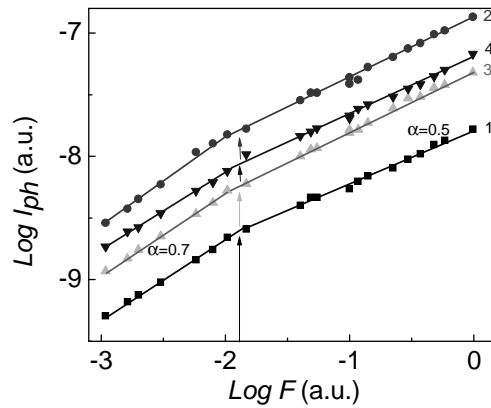


Fig.[7] Room temperature dependence of the photocurrent in amorphous $\text{Ge}_x\text{As}_x\text{Se}_{1-2x}$ thin films on the light intensity $\text{Log} I_{ph} = \text{Log} F$. x: 1-0.09; 2-0.14; 3-0.16; 4-0.30, the arrows indicate the mono- to bimolecular transition.

In our case the calculated temperature characteristics T^* for the low region of Lux-Ampere characteristics for amorphous $\text{Ge}_x\text{As}_x\text{Se}_{1-2x}$ thin films is $T^* = 383 \div 586$ K, which is in a good correlation with values obtained for vitreous As_2S_3 , As_2S_3 - Sb_2S_3 and $\text{AsS}_{1.5}\text{Ge}_x$ alloys [22]. Using the experimental data obtained from photoelectric measurements of amorphous $(\text{As}_4\text{S}_3\text{Se}_3)_{1-x}\text{Sn}_x$ - and $\text{Ge}_x\text{As}_x\text{Se}_{1-2x}$ thin films, a probably energy diagram model, including the localized states is proposed (Fig.8).

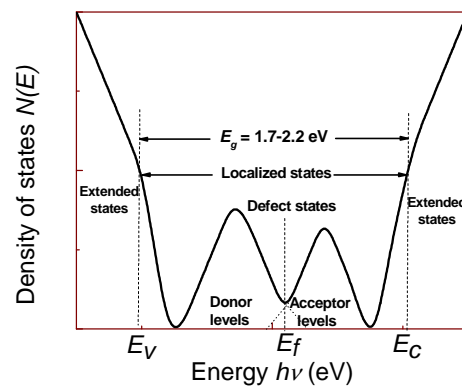


Fig.[8] The proposed appropriate energy band gap model for amorphous $(\text{As}_4\text{S}_3\text{Se}_3)_{1-x}\text{Sn}_x$ - and $\text{Ge}_x\text{As}_x\text{Se}_{1-2x}$ thin films.

From the experimental data of spectral distribution of photocurrent and dependence of the optical parameters on the composition of amorphous $\text{Ge}_x\text{As}_x\text{Se}_{1-2x}$ thin films (Fig.5), demonstrate the existence of some features in some compositions depending on average coordination number Z . That means in the forbidden gap of the amorphous material on the background of the exponential distribution of the localized states can be a lot of discrete levels with higher density of states induced by the fourth element (Sn or Ge) in the base glass. Some features and the existence of three distinct phases in the $\text{Ge}_x\text{As}_x\text{Se}_{1-2x}$ glassy system were established in [17-20].

In our previous paper [16] we also established two thresholds composition at concentration near $x=0.09$ and another near $x=0.16-0.18$, determined from the photocapacitance relaxation experiments in $\text{Ge}_x\text{As}_x\text{Se}_{1-2x}$ thin films.

SUMMARY

It was presented and discussed the experimental results on steady-state photoconductivity of amorphous $(\text{As}_4\text{S}_3\text{Se}_3)_{1-x}\text{Sn}_x$ and $\text{Ge}_x\text{As}_x\text{Se}_{1-2x}$ thin films. It was shown, that the spectral distribution of the stationary photoconductivity for both above-mentioned glass systems depends on the composition and polarity on the illuminated electrode. The experimental results are interpreted in framework of the multiple trapping models for amorphous materials, with exponential distribution of the localized states in the band gap. It was shown that the optical parameters determined from the photoelectrical characteristics depend on the composition with two thresholds characteristic, i.e. on the average coordination number Z . An appropriate energy band gap model is proposed.

ACKNOWLEDGEMENT

This work was supported by the project # 15.817.02.03A of the SCSTD of the ASM.

REFERENCES

1. Z. Tang, V.S. Shiryaev, D. Furniss, L. Sojka, S. Sujecki, T.M. Benson, A.B. Seddon, M.F. Churbanov, *Low loss Ge-As-Se chalcogenide glass fiber, fabricated using extruded perform, for mid-infrared photonics*, Optical Materials Express **5**(8), 1722-1737 (2015).
2. I. Blonskyi, V. Kadan, O. Shpotytuk, M. Iovu, P. Korenyuk, I. Dmitruk, *Filament-induced self-written waveguides in glassy $\text{As}_4\text{Ge}_{30}\text{S}_{66}$* , Applied Physics **B104**, 951-956 (2011).
3. A.V. Stronski, M. Vlcek, S.A. Kostyukevych, V.M. Tomchuk, E.V. Kostyukevych, S.V. Svechnikov, A.A. Kudreavtsev, N.L. Moskalenko, A.A. Koptyukh, *Study of non-reversible*

- photostructural transformations in $As_{40}S_{60-x}Se_x$ layers applied for fabrication of holographic protective elements*, Semiconductor Physics, Quantum Electronics & Optoelectronics, **5**(3), 284-287 (2002).
4. M. Reinfeld, J. Teteris, *Surface relief and polarization holographic formation in amorphous As-S-Se films*, Journal of Optoelectronics and Advanced Materials **13**(11-12), 1531-1533 (2011).
 5. R. Golovchak, O. Shpotyuk, M. Iovu, A. Kovalskiy, H. Jain, *Topology and chemical order in $As_xGe_xSe_{1-2x}$ glasses: A high-resolution X-ray photoelectron spectroscopy study*, J. of Non-Crystalline Solids **357**, 3454-3460 (2011).
 6. M.S. Iovu, S.D. Shutov, L. Toth, *Transient photocurrents under optical bias in time-of-flight experiments with amorphous films of $As_2Se_3:Sn$ and $As_2S_3:Sb_2S_3$* , Phys. Stat. Sol. (b), **195**, 149-157 (1996).
 7. M. Iovu, S. Shutov, *Tin-doped arsenic selenide glasses*, J. of Optoelect. and Adv. Mater., **1**(1), 27-36 (1999).
 8. M.S. Iovu, S.D. Shutov, V.I. Arkhipov, G.J. Adriaenssens, *Effect of Sn doping on the steady-state and transient photoconductivity in amorphous As-Se films*, Romanian Reports in Physics **51**(3-4), 297-308 (1999).
 9. M.S. Iovu, S.D. Shutov, V.I. Arkhipov, G.J. Adriaenssens, *Effect of Sn doping on photoconductivity in amorphous As_2Se_3 and AsSe films*, J. of Non-Crystalline Solids **299-302**, 1008-1012 (2002).
 10. D.V. Harea, I.A. Vasiliev, E.P. Colomeico, M.S. Iovu, *Persistent photoconductivity in amorphous As_2Se_3 films with Sn impurity*, J. of Optoelect. and Adv. Mater., **5**(5), 1115-1120 (2003).
 11. V.I. Arkhipov, M.S. Iovu, A.I. Rudenko, S.D. Shutov, *Multiple trapping model: approximate and exact solutions*, Solid State Commun., **62**(5), 339-340 (1987).
 12. M.A. Iovu, M.S. Iovu, S.D. Shutov, *Photoelectrical properties of the contact metall-vitreous As_2S_3 and Sb_2S_3* , JTF Letters **4**, 1246-1249 (1978).
 13. O.V. Iaseniuc, M.S. Iovu, I.A. Cojocaru, A.M. Prisacar, *Photoconductivity and light induced phenomena in amorphous $(As_4S_3Se_3)_{1-x}Sn_x$ thin films*, Moldavian Journal of the Physical Sciences **13**(2), 50-60 (2014).
 14. O.V. Iaseniuc, M.S. Iovu, I.A. Cojocaru, A.M. Prisacar, *Steady-state photoconductivity of amorphous $(As_4S_3Se_3)_{1-x}Sn_x$ films*, Proc. SPIE **9258**, 92580M (2015).
 15. M.S. Iovu, S.D. Shutov, A.M. Andriesh, E.I. Kamitsos, C.P.E. Varsamis, D. Furniss, A.B. Seddon, M. Popescu, *Spectroscopic studies of bulk As_2S_3 glasses and amorphous films doped with Dy, Sm and Mn*, J. of Optoelect. and Adv. Mater., **3**(2), 443-454 (2001).
 16. I.A. Vasiliev, M.S. Iovu, E.P. Colomeico, *Photocapacitance relaxation and rigidity transition in $Ge_xAs_xSe_{1-2x}$ amorphous films*, Moldavian Journal of the Physical Sciences **10**(2), 5-9 (2011).
 17. M.F. Thorpe, D.J. Jacobs, M.V. Chubynsky, J.C. Phillips, *Self-organization in network glasses*, J. of Non-Cryst. Solids **266-269**, 859-866 (2000).
 18. Y. Wang, P. Boolchand, M. Micoulaut, *Glass structure, rigidity transitions and the intermediate phase in the Ge-As-Se ternary*, Europhys. Lett., **52**(6), 633-639 (2000).
 19. Qu Tao, D.G. Georgiev, P. Boolchand, M. Micoulaut, *The intermediate phase in ternary $Ge_xAs_xSe_{1-2x}$ glasses*, Mat. Res. Soc. Symp. Proc., **754**, CC8-12 (2003).
 20. O. Shpotyuk, M. Hyla, V. Boyko, R. Golovchak, *Reversibility windows in selenide-based chalcogenide glasses*, Physica B **403**, 3830-3837 (2008).
 21. A. Rose, "Concepts in photoconductivity and allied problems", Interscience Publishers, New York-London, 168 (1963).
 22. M. Popescu, A. Andriesh, V. Ciumas, M. Iovu, S. Sutov, D. Tiuleanu, "Physics of chalcogenide glasses", Editura stiintifica Bucuresti – I.E.P. Stiinta, Chisinau, 485 (1996).
 23. N. Qamhieh, G.J. Adriaenssens, *Steady-state photoconductivity in amorphous germanium selenide films*, J. of Non-Crystalline Solids **292**, 80-87 (2001).